Research Article
NAFLD and Alcohol-Related Liver Diseases

JOURNAL
OF HEPATOLOGY

Inhibition of ATG3 ameliorates liver steatosis by increasing mitochondrial function

Graphical abstract

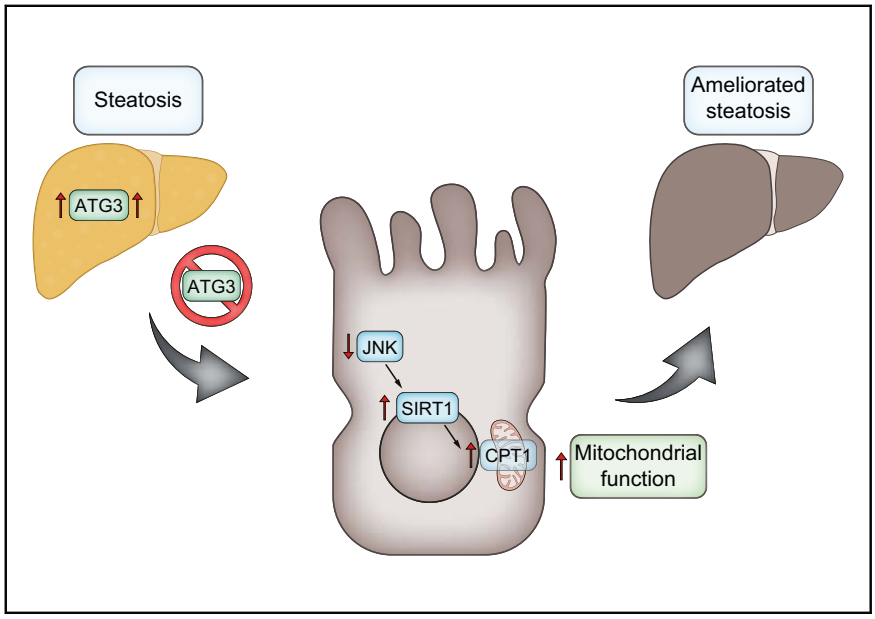

Highlights

- ATG3 levels are elevated in the livers of mice and patients with NAFLD.
- Inhibition of ATG3 in human hepatocytes and in mouse liver ameliorates steatosis by stimulating SIRT1, CPT1a, and mitochondrial function.
- Hepatic knockdown of SIRT1 or CPT1a blunts the ability of ATG3 inhibition to increase mitochondrial activity and to alleviate steatosis.

Authors

Natália da Silva Lima, Marcos F. Fondevila, Eva Nóvoa, …, Agueda Gonzalez-Rodriguez, Patricia Aspichueta, Ruben Nogueiras

Correspondence

ruben.nogueiras@usc.es (R. Nogueiras).

Lay summary

We show that autophagy-related gene 3 (ATG3) contributes to the progression of non-alcoholic fatty liver disease in humans and mice. Hepatic knockdown of ATG3 ameliorates the development of NAFLD by stimulating mitochondrial function. Thus, ATG3 is an important factor implicated in steatosis.

https://doi.org/10.1016/j.jhep.2021.09.008
 J. Hepatol. 2022, 76, 11–24

Research Article
NAFLD and Alcohol-Related Liver Diseases

JOURNAL OF HEPATOLOGY

Inhibition of ATG3 ameliorates liver steatosis by increasing mitochondrial function

Natália da Silva Lima[1,†], Marcos F. Fondevila[1,2,†], Eva Nóvoa[1,†], Xabier Buqué[3,4], Maria Mercado-Gómez[5], Sarah Gallet[6], Maria J. González-Rellan[1], Uxia Fernandez[1], Anne Loyens[6], Maria Garcia-Vence[7], Maria del Pilar Chantada-Vazquez[7], Susana B. Bravo[7], Patricia Marañon[8], Ana Senra[1], Adriana Escudero[1], Magdalena Leiva[9], Diana Guallar[10], Miguel Fidalgo[1], Pedro Gomes[11,12,13], Marc Claret[14,15], Guadalupe Sabio[9], Marta Varela-Rey[5,16], Teresa C. Delgado[5], Rocio Montero-Vallejo[17], Javier Ampuero[17], Miguel López[1,2], Carlos Diéguez[1,2], Laura Herrero[2,18], Dolors Serra[2,18], Markus Schwaninger[19], Vincent Prevot[6], Rocio Gallego-Duran[14,20], Manuel Romero-Gomez[17,20], Paula Iruzubieta[21], Javier Crespo[21], Maria L. Martinez-Chantar[5,20], Carmelo Garcia-Monzon[8,20], Agueda Gonzalez-Rodriguez[8,22], Patricia Aspichueta[3,4,20], Ruben Nogueiras[1,2,*]

[1]Department of Physiology, CIMUS, University of Santiago de Compostela-Instituto de Investigación Sanitaria, Santiago de Compostela, Spain; [2]CIBER Fisiopatologia de la Obesidad y Nutrición (CIBERobn), Spain; [3]Department of Physiology, University of the Basque Country UPV/EHU, Spain; [4]Biocruces Bizkaia Health Research Institute, Spain; [5]Liver Disease Lab, Center for Cooperative Research in Biosciences (CIC bioGUNE), Basque Research and Technology Alliance (BRTA), 48160 Derio, Bizkaia, Spain; [6]Univ. Lille, Inserm, CHU Lille, Laboratory of Development and Plasticity of the Neuroendocrine Brain, Lille Neuroscience & Cognition, UMR-S 1172, European Genomic Institute for Diabetes (EGID), F-59000 Lille, France; [7]Proteomic Unit, Health Research Institute of Santiago de Compostela (IDIS), Santiago de Compostela, 15705 A Coruña, Spain; [8]LiverResearchUnit, Santa Cristina University Hospital, Instituto de Investigación Sanitaria Princesa, Madrid, Spain; [9]Centro Nacional de Investigaciones Cardiovasculares (CNIC), Madrid, Spain; [10]Department of Biochemistry, CIMUS, University of Santiago de Compostela-Instituto de Investigación Sanitaria, Santiago de Compostela, Spain; [11]Department of Biomedicine, Unit of Pharmacology and Therapeutics, Faculty of Medicine, University of Porto, Porto, Portugal; [12]Coimbra Institute for Clinical and Biomedical Research (iCBR), Faculty of Medicine, University of Coimbra, Coimbra, Portugal; [13]Institute of Pharmacology and Experimental Therapeutics, Coimbra Institute for Clinical and Biomedical Research(iCBR), Faculty of Medicine, University of Coimbra, Coimbra, Portugal; [14]Neuronal Control of Metabolism (NeuCoMe) Laboratory, Institut d'Investigacions Biomèdiques August Pi iSunyer (IDIBAPS), 08036, Barcelona, Spain; [15]CIBER de Diabetes y Enfermedades Metabólicas Asociadas (CIBERDEM), 08036, Barcelona, Spain; [16]Gene Regulatory Control in Disease, CIMUS, University of Santiago de Compostela, Santiago de Compostela, Spain; [17]UGC Aparato Digestivo, Instituto de Biomedicina de Sevilla. Hospital Universitario Virgen del Rocío, Universidad de Sevilla, Sevilla, Spain; [18]Department of Biochemistry and Physiology, School of Pharmacy and Food Sciences, Institut de Biomedicina de la Universitat de Barcelona (IBUB), Barcelona, Spain; [19]University of Lübeck, Institute for Experimental and Clinical Pharmacology and Toxicology, Lübeck, Germany; [20]CIBER Enfermedades Hepáticas y Digestivas (CIBERehd), Spain; [21]Gastroenterology and Hepatology Department, Marqués de Valdecilla University Hospital. Clinical and Translational Digestive Research Group, IDIVAL, Santander, Spain; [22]CIBER de Diabetes y Enfermedades Metabólicas Asociadas (CIBERdem), Spain

Background & Aims: Autophagy-related gene 3 (ATG3) is an enzyme mainly known for its actions in the LC3 lipidation process, which is essential for autophagy. Whether ATG3 plays a role in lipid metabolism or contributes to non-alcoholic fatty liver disease (NAFLD) remains unknown.

Methods: By performing proteomic analysis on livers from mice with genetic manipulation of hepatic p63, a regulator of fatty acid metabolism, we identified ATG3 as a new target downstream of p63. ATG3 was evaluated in liver samples from patients with NAFLD. Further, genetic manipulation of *ATG3* was performed in human hepatocyte cell lines, primary hepatocytes and in the livers of mice.

Results: ATG3 expression is induced in the liver of animal models and patients with NAFLD (both steatosis and non-alcoholic steatohepatitis) compared with those without liver disease. Moreover, genetic knockdown of *ATG3* in mice and human hepatocytes ameliorates p63- and diet-induced steatosis, while its overexpression increases the lipid load in hepatocytes. The inhibition of hepatic ATG3 improves fatty acid metabolism by reducing c-Jun N-terminal protein kinase 1 (JNK1), which increases sirtuin 1 (SIRT1), carnitine palmitoyltransferase 1a (CPT1a), and mitochondrial function. Hepatic knockdown of SIRT1 and CPT1a blunts the effects of ATG3 on mitochondrial activity. Unexpectedly, these effects are independent of an autophagic action.

Conclusions: Collectively, these findings indicate that ATG3 is a novel protein implicated in the development of steatosis.

Lay summary: We show that autophagy-related gene 3 (ATG3) contributes to the progression of non-alcoholic fatty liver disease

Keywords: ATG3; sirtuin 1; lipid metabolism; NAFLD; NASH; mitochondria.
Received 18 March 2021; received in revised form 3 August 2021; accepted 13 September 2021; available online 21 September 2021

* Corresponding author. Address: Department of Physiology, Research Centre of Molecular Medicine and Chronic Diseases (CIMUS), Instituto de Investigación Sanitaria de Santiago de Compostela, Universidadde Santiago de Compostela (USC), Santiago de Compostela, Spain.
E-mail address: ruben.nogueiras@usc.es (R. Nogueiras).
† Contributed equally

https://doi.org/10.1016/j.jhep.2021.09.008

in humans and mice. Hepatic knockdown of ATG3 ameliorates the development of NAFLD by stimulating mitochondrial function. Thus, ATG3 is an important factor implicated in steatosis.

Introduction

Non-alcoholic fatty liver disease (NAFLD) is a major health threat in both developed and developing countries and is a precursor of the more advanced liver diseases, including non-alcoholic steatohepatitis (NASH), cirrhosis, and liver cancer. Currently, understanding the multiple and complex molecular pathways implicated in NAFLD onset and progression is a major priority.

The transcription factor p63, which belongs to a family comprising p53, p63, and p73,[1] is one of many factors that contributes to the development of liver steatosis. The role of p63 as a tumor suppressor and in cell maintenance and renewal is well studied, but we have recently reported that it is also relevant in the control of lipid metabolism.[2] p63 encodes multiple isoforms that can be grouped into 2 categories; isoforms with an acidic transactivation domain (TA) and those without this domain (domain negative). The TAp63α isoform is elevated in the liver of animal models of NAFLD as well as in liver biopsies from obese patients with NAFLD. Furthermore, downregulation of p63α in the liver attenuates liver steatosis in diet-induced obese (DIO) mice, while the activation of TAp63α increases hepatic fat content, mediated by the activation of IKKβ and endoplasmic reticulum stress.[2]

A specialized form of autophagy that degrades lipid droplets, termed "lipophagy", is a major pathway of lipid mobilization in hepatocytes. Lipophagy is elevated in hepatoma cells upon exposure to free fatty acids,[3] and reduces the fatty acid load in mouse hepatocytes.[4] Its impairment has been associated with the development of fatty liver and insulin resistance[3,5]; in contrast, the autophagic flux is increased during the activation of hepatic stellate cells.[6]

In the present study, we used an unbiased proteomics approach to gain insight into novel proteins modulating lipid metabolism in the liver of mice with genetic knockdown or overexpression of TAp63α. We found that autophagy-related gene 3 (ATG3) was upregulated by TAp63α activation and downregulated after p63α inhibition. ATG3 is elevated in several animal models of NAFLD and in the liver of patients with NAFLD. Genetic overexpression of ATG3 increased the lipid load in hepatocytes, while its repression alleviated TAp63α- and diet-induced steatosis. ATG3 exerted its role in lipid metabolism by regulating SIRT1 and mitochondrial function. Collectively, these findings identify ATG3 as a novel factor implicated in the development of steatosis.

Materials and methods

Animals and diets

Mouse experiments were conducted to the standard protocols approved by the Animal Ethics Committee at the University of Santiago de Compostela, and mice received the highest levels of human care. C57BL/6J (8-week-old male) mice were housed in rooms under constant temperature (22°C), a 12:12 h light/dark cycle and with *ad libitum* access to standard diet (SD) (U8200G10R, SAFE), a choline-deficient high-fat diet (CDHFD) (D05010402; 45 kcal% fat, Research Diets), a methionine- and choline-deficient diet (A02082002BR, Research Diets), or a high-fat diet (HFD) (D12492; 60 kcal% fat, Research Diets) used during specified times and experiments. Food intake and body weight were measured weekly during all experimental phases.

Cohort of patients with NAFLD

The study population included 55 patients with biopsy-proven NAFLD (25 with non-alcoholic fatty liver [NAFL], and 30 with NASH), who underwent a liver biopsy during bariatric surgery or with a diagnostic purpose at the Santa Cristina University Hospital (Madrid, Spain) and at the Marqués de Valdecilla University Hospital (Santander, Spain) (Table S1). Liver samples with histologically normal liver obtained from 32 individuals during programmed cholecystectomy without steatosis were selected as healthy controls. Patients consumed <20 g of alcohol/day, did not take potentially hepatotoxic drugs, had no analytical evidence of iron overload, and were seronegative for autoantibodies and for hepatitis B/C viruses and human immunodeficiency virus. Hepatic histopathological analysis was performed according to the scoring system of Kleiner *et al.*[7] Minimal criteria for NASH included the combined presence of grade 1 steatosis, hepatocellular ballooning, and lobular inflammation with or without fibrosis. This study was performed in agreement with the Declaration of Helsinki and with local and national laws. The Human Ethics Committees of the 2 hospitals approved the study procedures, and all participants voluntarily signed an informed written consent before inclusion in the study.

Results

Hepatic ATG3 is regulated by p63 and increased in diet-induced animal models of steatosis

Hepatic overexpression of TAp63α isoform induces steatosis, while inhibition of p63α ameliorates diet-induced steatosis.[2] Proteomic analyses in the liver of these 2 animal models identified novel pathways and regulators of hepatic lipid accumulation (Fig. 1A-1D). Volcano plots show that multiple changes in hepatic protein levels were triggered by the manipulation of p63 (Fig. 1A-B). We specifically searched for proteins oppositely expressed in mice following the overexpression or knockdown of p63; we found that p63 positively regulated 43 proteins. Analyzing this protein set revealed a significant overrepresentation (44%) of metabolism-related proteins, with mitochondria identified as the most affected cell component (Fig. 1C). A heatmap showed several proteins involved in lipid metabolism with a strong positive regulation by p63 overexpression, including ATG3 (Fig. 1D). Given the relevant role of lipophagy in regulating fatty acid metabolism, and that ATG3 has not previously been related to liver function, we selected this candidate for further investigation. We corroborated that ATG3 mRNA expression and protein levels were upregulated when TAp63α was induced in the liver, while it was reduced when hepatic p63α was inhibited in DIO mice (Fig. 1E).

Next, we evaluated the expression of ATG3 in livers from mouse models of diet-induced NAFLD and NASH, including mice fed a HFD or a CDHFD, and found that *ATG3* mRNA was elevated (Fig. 1F). Together, these results indicate that ATG3 expression is consistently increased in preclinical models of steatosis and steatohepatitis.

ATG3 is increased in the livers of patients with NAFLD

ATG3 expression was evaluated in liver biopsies from patients with NAFLD or healthy livers (Table S1). *ATG3* mRNA expression

was significantly higher in the livers of patients with NAFLD (both NAFL and NASH) than in those from patients without the disease (Fig. 2A). ATG3 positively correlated with steatosis grade (Fig. 2B), NAFLD activity score (Fig. 2C), and fatty liver index (Fig. 2D). ATG3 levels were increased in obese (BMI>30) *vs.* non-obese (BMI<30) patients (Fig. 2E), and positively correlated with BMI (Fig. 2F). Altogether, these results indicate that higher ATG3 levels are present in patients with NAFLD.

ATG3 increases lipid content and reduces β-oxidation in human hepatocytes

ATG3 mRNA expression (Fig. 3A) and lipid content (Fig. 3B) were increased in human hepatic THLE2 cells treated with oleic acid (OA). However, small-interfering (si)RNA-mediated ATG3 silencing reduced OA-induced lipid storage (Fig. 3B and Fig. S1A). As previously reported,[2] TAp63α overexpression increased the lipid droplets in hepatocytes, but this effect was blunted when ATG3 was silenced (Fig. 3C). The transfection efficiency of the plasmid for p63, and siRNA for ATG3, were corroborated (Fig. S1B). ATG3 overexpression (Fig. S1C) increased the lipid content in THLE2 cells (Fig. 3D). Importantly, similar loss- and gain-of-function experiments in another human hepatic cell line, HepG2, provided the same results: the OA-induced lipid content was reduced when ATG3 was silenced (Fig. 3E), while ATG3 overexpression augmented the lipid load (Fig. S1D and Fig. 3F). The rate of fatty acid β-oxidation, assessed using ^{14}C-palmitate, was decreased upon ATG3 overexpression (Fig. 3G). Finally, we isolated hepatocytes from mice and transfected them with siATG3 and phosphorylated ATG3 (Fig. S1E-S1F) and detected an increase and reduction of fatty acid β-oxidation, respectively, in hepatocytes previously incubated with OA (Fig. 3H-3I).

ATG3 regulates mitochondrial activity in hepatocytes

The overexpression of ATG3 in HepG2 cells decreased oxygen consumption rate (Fig. 4A). More specifically, basal respiration, ATP-linked respiration, proton leak, maximal respiration, spare capacity, and 24 h non-mitochondrial oxygen consumption were decreased after ATG3 overexpression (Fig. 4A). These results were consistent with reduced protein levels of the mitochondrial complexes II (II-SDHB), III, and V (Fig. 4B). No changes were observed in protein levels of fatty acid synthase (FAS), acetyl CoA carboxylase, or carnitine palmitoyltransferase 1a (CPT1a) (Fig. 4C). However, the induction of ATG3 decreased peroxisome proliferator-activated receptor gamma coactivator 1 alpha (PGC1α) and sirtuin 1 (SIRT1) (Fig. 4D), 2 proteins that promote mitochondrial function and fatty acid oxidation.[8] These results were corroborated in isolated hepatocytes, where the overexpression of ATG3 (Fig. S1E) also reduced protein levels of SIRT1 and PGC1α (Fig. 4E).

ATG3 inhibition in HepG2 cells increased the oxygen consumption rate, with significant stimulation of basal respiration, ATP-linked respiration, proton leak, maximal respiration, and non-mitochondrial oxygen consumption (Fig. 4F). This was in agreement with increased levels of mitochondrial complexes I, II (II-SDHB), and IV (IV-COX II) (Fig. 4G), and the upregulation of CPT1a, PGC1α and SIRT1 levels after silencing ATG3 (Fig. 4H, 4I). The inhibition of ATG3 (Fig. S1F) also increased protein levels of SIRT1 and PGC1α in primary mouse hepatocytes (Fig. 4J). All results obtained in HepG2 cells were also corroborated in THLE2 cells (Fig. S2).

Inhibition of hepatic ATG3 ameliorates CDHFD-induced steatosis

We next investigated the *in vivo* relevance of these findings. Mice were fed a CDHFD for 16 weeks; at week 8, mice were injected in the tail vein with a lentivirus encoding for a scrambled short-hairpin (sh)RNA or shRNA against ATG3. No differences in body weight or feeding were observed (Fig. 5A-5B). Hepatic ATG3 was decreased after the lentiviral injection (Fig. 5C). Although the liver mass and circulating triglycerides and non-esterified fatty acids were not affected by ATG3-knockdown (Fig. 5D and Table S2), circulating aspartate aminotransferase (AST) and alanine aminotransferase (ALT) were significantly lower (Fig. 5E). Consistent with this, hepatic triglyceride content and Oil Red O staining in liver sections of mice after ATG3-knockdown showed a lower amount of lipids, with no differences in fibrotic content (Sirius Red staining) (Fig. 5F). ATG3 inhibition increased CPT1a, PGC1α, and SIRT1 (Fig. 5G-5H), as well as the mitochondrial complexes I (I-NDUFB8) and II (II-SDHB) (Fig. 5I) and the activity of mitochondrial complex II (Fig. 5J). Functional assays revealed an increased β-oxidation rate in livers of mice with ATG3-knockdown (Fig. 5K). These effects were independent of cellular proliferation since the expression of cyclin D1 and cyclin D2 and the immunostaining of Ki67 were unchanged between the groups (Fig. S3A-S3B). The knockdown of ATG3 did not affect mRNA expression of fibrotic markers (Fig. S4A).

Inhibition of hepatic ATG3 ameliorates TAp63α-induced steatosis

We next evaluated the effects of ATG3 inhibition on TAp63α-induced steatosis in mice. For this, mice fed a SD were injected via the tail vein with adeno-associated virus (AAV)8-TAp63α or AAV8-GFP; and then, after 8 weeks, they were injected again with either shATG3 (to knockdown ATG3) or scrambled shRNA (as a control) and maintained on the same diet for another 8 weeks. Body weight (Fig. 6A) and food intake (Fig. 6B) remained unchanged. Administration of AAV8-TAp63α or lentivirus-shATG3 caused an increase in p63 and a decrease in ATG3, respectively (Fig. 6C). Even though liver mass was unchanged (Fig. 6D), higher circulating AST and ALT levels were observed after TAp63α overexpression; ATG3 inhibition reduced AST and ALT levels (ALT was not statistically significant; $p = 0.0513$) (Fig. 6E). Serum triglycerides and non-esterified fatty acids were similar among all groups (Table S3).

As previously reported,[2] the overexpression of TAp63α caused liver steatosis, an effect that was blunted by ATG3-knockdown (Fig. 6F). Mechanistically, AAV8-TAp63α-treated mice had elevated levels of the FAS protein and reduced CPT1a, PGC1α, and SIRT1 (Fig. 6G-H). ATG3 inhibition restored the levels of CPT1a, PGC1α, and SIRT1 to those of the control group (Fig. 6G-6H). Hepatic overexpression of TAp63α decreased the levels of all mitochondrial complexes, while ATG3 inhibition normalized the liver levels of complexes I and II (Fig. 6I). In these groups, mRNA expression of fibrotic markers such as collagen alpha 2, collagen III or αSMA remained unaltered, although collagen alpha 1 was

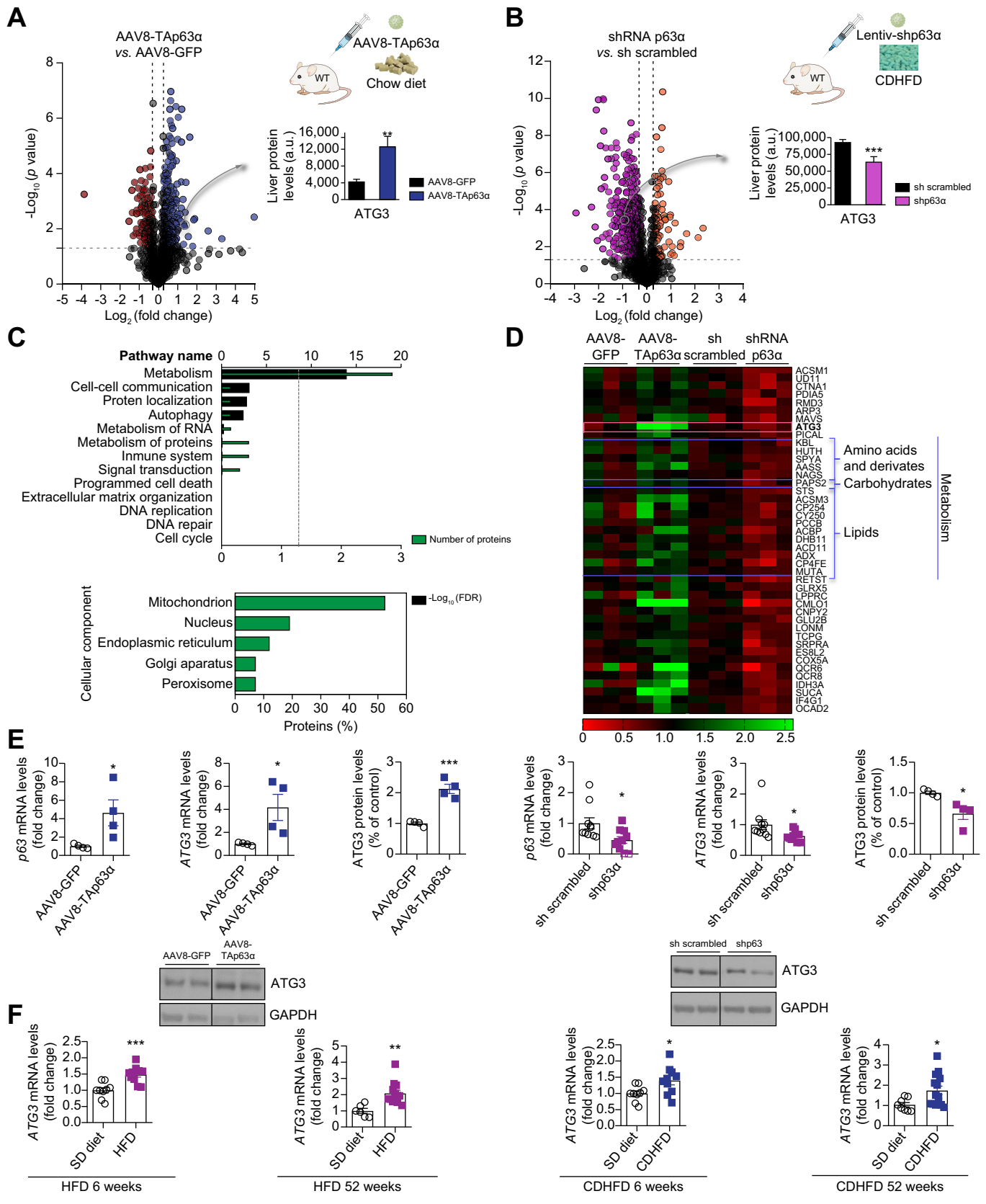

Fig. 1. Hepatic ATG3 is upregulated in different mouse models of NAFLD. (A, B) Volcano plots of hepatic protein expression determined by LC-MS/MS proteomics of (A) mice fed a SD, with TAp63α overexpressed specifically in liver compared to the control group (n = 3 per group). Upregulated proteins (blue) and downregulated proteins (brown); or (B) mice fed a CDHFD for 12 weeks, with hepatic p63α downregulated as compared to the control group (n = 3 per group). Upregulated proteins (orange) and downregulated (violet). Values obtained for ATG3 are represented in the bar graph. (C) Reactome pathway classification of

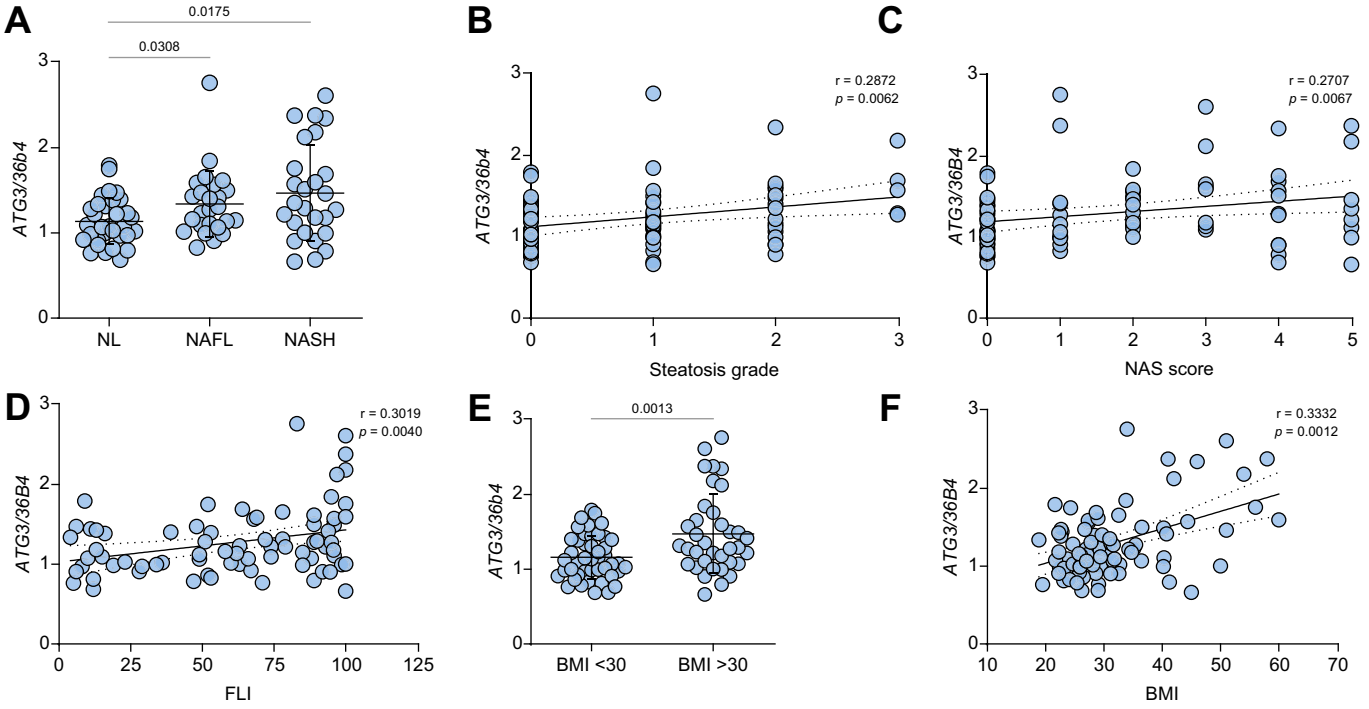

Fig. 2. ATG3 is increased in the liver of patients with NAFLD. (A) *ATG3* mRNA expression in the liver of patients without NAFLD (NL) (n = 32), with NAFL (n = 25) or NASH (n = 30). (B) Correlation between ATG3 and steatosis grade. (C) Correlation between ATG3 and NAS score. (D) Correlation between ATG3 and fatty liver index. (E) *ATG3* mRNA expression in the liver of non-obese *vs.* obese patients with NAFLD. (F) Correlation between ATG3 and body mass index. HPRT was used to normalize mRNA levels. Data are presented as mean ± standard deviation. *p* value using a Student's *t* test (B) (C) (D) (E) (F) or one-way ANOVA followed by a Newman-Keuls multiple comparison test (A). FLI, fatty liver index; NAFL, non-alcoholic fatty liver; NAFLD, non-alcoholic fatty liver disease; NAS, NAFLD activity score; NASH, non-alcoholic steatohepatitis; NL, normal liver.

elevated by TAp63α and reduced when ATG3 was inhibited (Fig. S4B).

Knockdown of hepatic ATG3 does not affect fibrosis

We next evaluated whether ATG3-knockdown in liver alleviates fibrosis by injecting mice via the tail vein with a lentivirus shATG3 or shRNA-scrambled (as control); mice were fed a SD for 4 week and a methionine- and choline-deficient diet for another 4 weeks to induce fibrosis, and were sacrificed at week 8.[9] Body weight was similar between ATG3-knockdown and control mice (Fig. S5A). As expected, ATG3-knockdown significantly reduced *ATG3* mRNA (Fig. S5B). No differences were observed for liver mass (Fig. S5C), serum AST or ALT (Fig. S5D), inflammatory or profibrotic markers (Fig. S5E), or Oil Red O or Sirius Red staining (Fig. S5F). Of note, ATG3 was highly expressed in isolated hepatic stellate cells compared to hepatocytes or Kupffer cells (Fig. S6A) and in LX2 cells (a human hepatic stellate cell line) compared to THLE2 and HepG2 cells (Fig. S6B). However, the treatment of LX2 cells with TGFβ did not change ATG3 expression, and the TGFβ-induced expression of fibrotic markers was not affected after silencing ATG3 (Fig. S6C-S6D).

ATG3 requires SIRT1 to modulate lipid metabolism and mitochondrial activity

We next assessed the functional relevance of SIRT1 as a potential modulator of ATG3. Similar to the results shown in Fig. 3B, silencing ATG3 in HepG2 cells ameliorated OA-induced lipid load (Fig. S7A). However, when SIRT1 was also silenced, siATG3 failed to decrease OA-induced lipid content (Fig. S7A). These results were also corroborated in THLE2 cells co-transfected with siATG3 and siSIRT1 (Fig. S7B). Moreover, the higher oxygen consumption rate induced by siATG3 in THLE2 cells was also lost after SIRT1 silencing (Fig. S7C). In addition, ATG3-induced lipid content was blunted by resveratrol, a pharmacological activator of SIRT1 in both THLE2 cells (Fig. S8A) and primary hepatocytes (Fig. S8B). In isolated hepatocytes, ATG3 also reduced the oxygen consumption rate while resveratrol blunted this effect (Fig. S8C). In line with these results, silencing ATG3 increased SIRT1 activity and reduced acetylated levels of PGC1α, while its overexpression reduced SIRT1 activity in isolated hepatocytes (Fig. S9A-S9C).

Next, we evaluated the *in vivo* relevance of SIRT1 as a mediator of the effects of ATG3. For this, mice fed a CDHFD were injected with a lentivirus encoding either a scrambled shRNA (as

deregulated proteins in liver of mice from (A) and (B), showing the number of proteins included in each category and the associated FDR. The same proteins were also classified according to the cellular component using FunRich tool. (D) Heatmap representation of protein levels differentially expressed in the groups from (A) and (B). (E) mRNA levels of *p63* and *ATG3*, as well as ATG3 protein levels, in mice in the conditions as in (A) and (B). (n = 4 per group). (F) *ATG3* mRNA in liver of mice fed a SD, an HFD, or a CDHFD (n = 9–14 per group). HPRT and GAPDH were used to normalize mRNA and protein levels, respectively. Lines indicate splicing in the same gel. Data are presented as mean ± SEM; **p* <0.05, ***p* <0.01, ****p* <0.001, using a Student's *t* test. AAV, adeno-associated virus; CDHFD, choline-deficient high-fat diet; FDR, false discovery rate; HFD, high-fat diet; LC-MS/MS, liquid chromatography tandem mass spectrometry; NAFLD, non-alcoholic fatty liver disease; SD, standard diet; sh(RNA), short-hairpin (RNA); WT, wild-type.

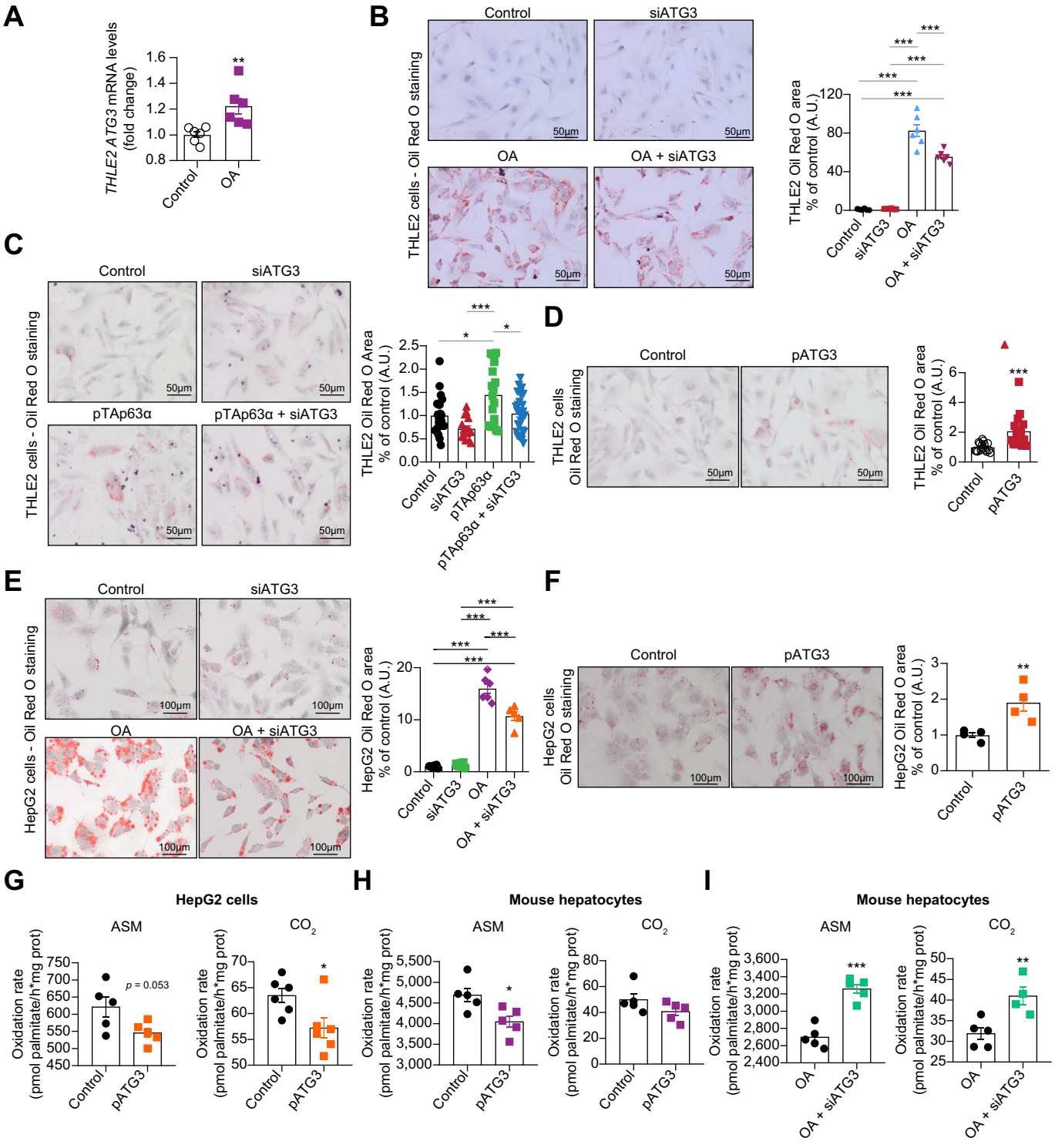

Fig. 3. ATG3 regulates lipid accumulation in human hepatic cell lines. (A) *ATG3* mRNA in THLE2 cells treated with OA (1 mM) for 24 h (n = 6 per group). (B–F) Representative Oil Red O staining of (B) THLE2 cells with siATG3 treated with OA or vehicle (n = 6 per group); (C) TAp63α-upregulated THLE2 cells after ATG3 silencing (n = 15 per group); and (D) THLE2 cells with overexpression of ATG3 (n = 12 per group). (E, F) Representative Oil Red O staining of HepG2 cells with ATG3 downregulated (E) or ATG3 overexpressed (F), treated with OA or vehicle for 24 h (n = 4–7 per group). (G) Palmitate oxidation rate (partial and complete oxidation) in HepG2 cells overexpressing ATG3. Palmitate oxidation rate in mouse hepatocytes after overexpression (H) and inhibition (I) of ATG3. The n represents the number of independent experiments. Data are presented as mean ± SEM; *p <0.05, **p <0.01, ***p <0.001, using a Student's t test (A) (D) (F) (G) or one-way ANOVA followed by a Newman-Keuls multiple comparison test (B) (C) (E). ASM, acid soluble metabolites; OA, oleic acid; si(RNA), small-interfering RNA; TA, transactivation domain.

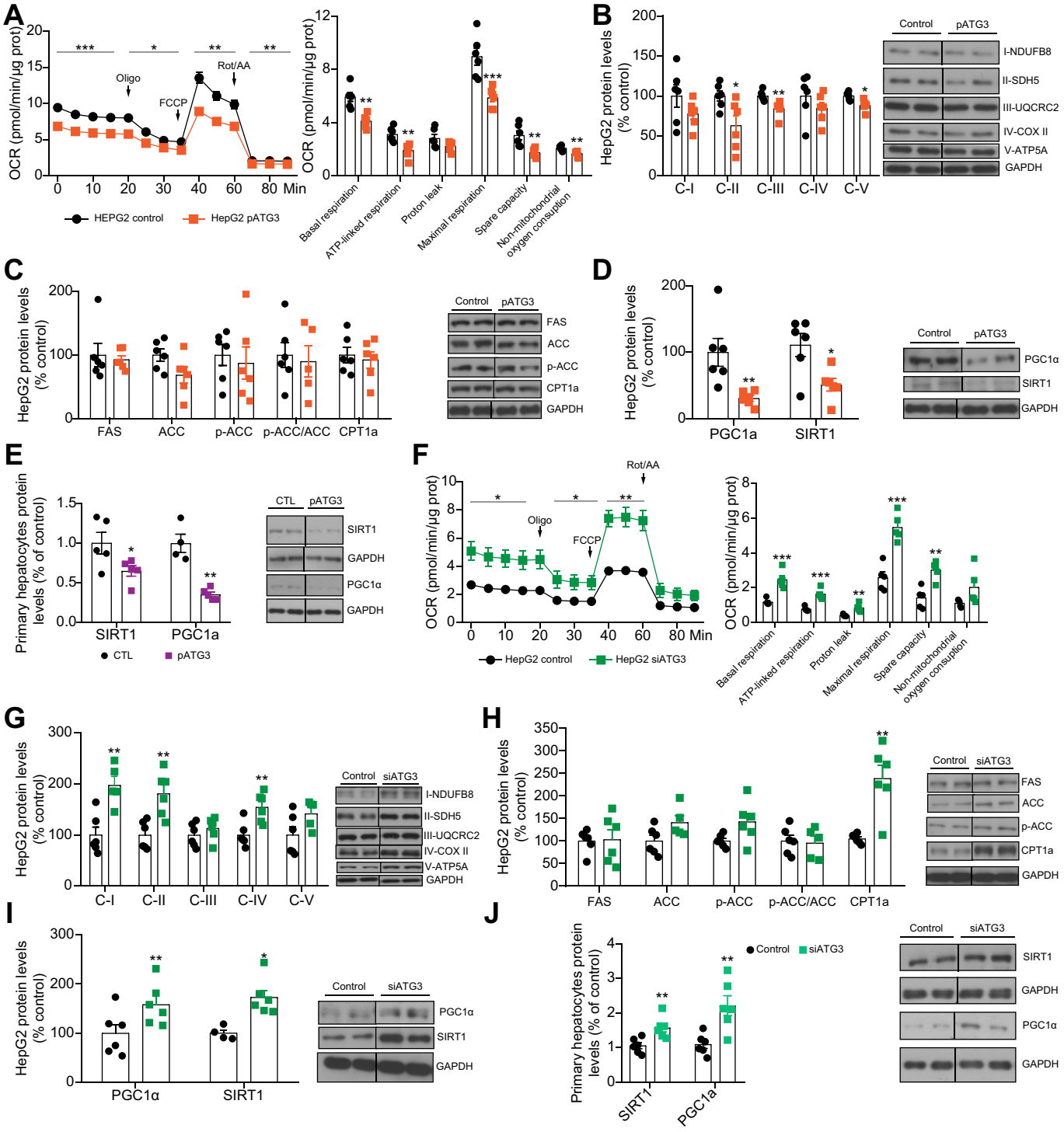

Fig. 4. ATG3 modulates mitochondrial function in hepatocytes. HepG2 cells overexpressing ATG3 were analyzed for (A) OCR, (B) protein levels of OXPHOS complex subunits I–V, (C) lipid metabolism markers, and (D) protein levels of PGC1α and SIRT1 (n = 6 per group). (E) PGC1α and SIRT1 protein levels of primary mouse hepatocytes overexpressing ATG3 (n = 5 per group). ATG3-silenced HepG2 cells were analyzed for (F) OCR, (G) protein levels of OXPHOS complex subunits I–V, (H) lipid metabolism markers, and (I) protein levels of PGC1α and SIRT1 (n = 5–6 per group). (J) PGC1α and SIRT1 protein levels of ATG3-silenced primary mouse hepatocytes (n = 6 per group). The n represents the number of independent experiments. GAPDH was used to normalize protein levels. Dividing lines indicate splicing in the same gel. Data are presented as mean ± SEM; *p <0.05, **p <0.01, ***p <0.001, using a Student's t test. OCR, oxygen consumption rate; OXPHOS, oxidative phosphorylation.

a control) or shRNA-ATG3. At week 4, a second lentiviral vector with shRNA-scrambled or shRNA-SIRT1 was injected; and mice were sacrificed at week 8. Body weight and food intake remained unchanged (Fig. 7A-7B). ATG3 and SIRT1 were reduced in liver after the injections of shRNA-ATG3 and shRNA-SIRT1, respectively (Fig. 7C). Even though liver weight was not affected, AST and ALT were reduced after ATG3-knockdown, and this reduction was abolished when both ATG3 and SIRT1 were silenced

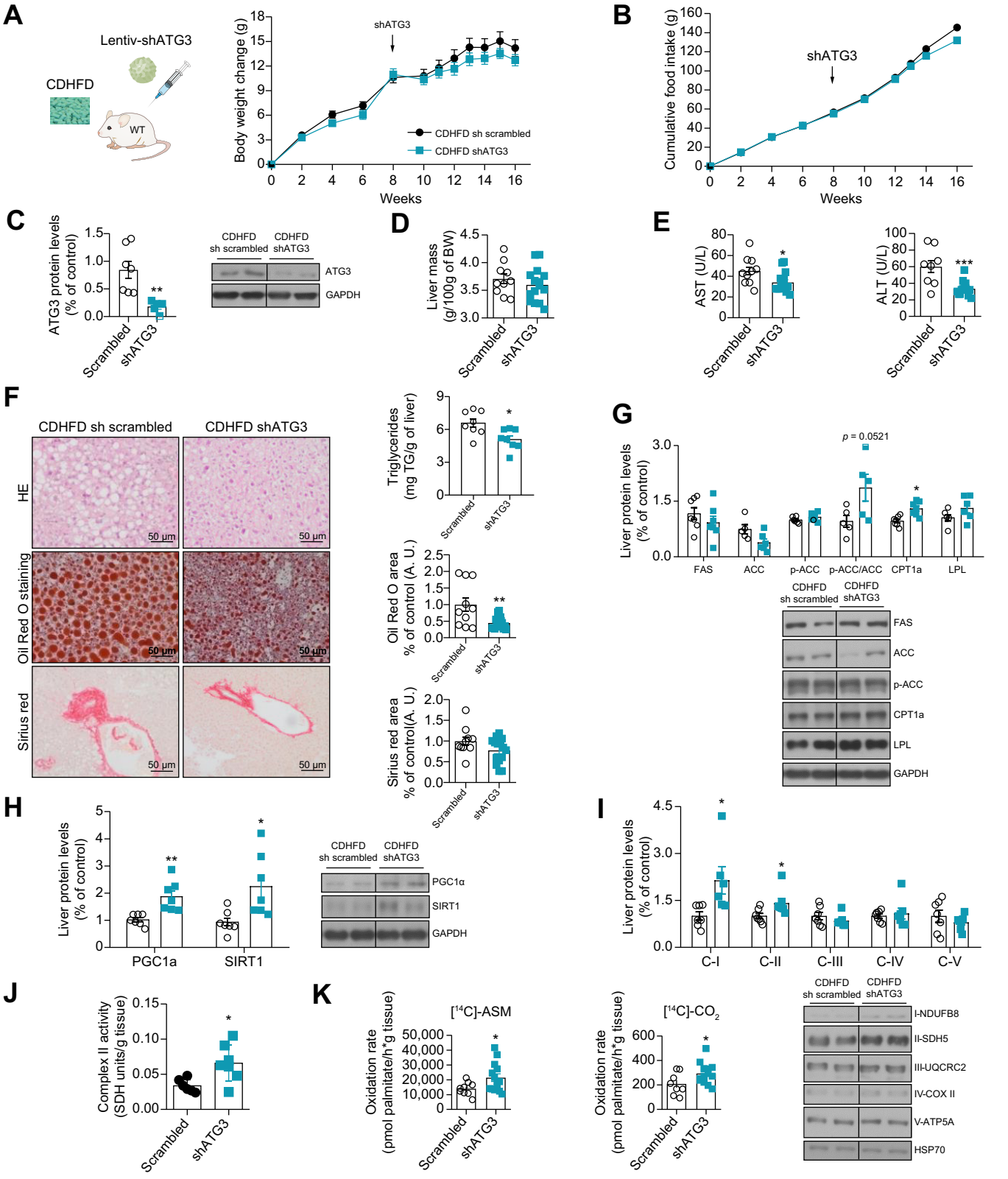

Fig. 5. Liver-specific downregulation of ATG3 ameliorates NAFLD induced by CDHFD. (A) Body weight change, (B) food intake, (C) hepatic ATG3 protein levels, and (D) liver mass of mice fed CDHFD for 16 weeks, with lentivirus of shRNA ATG3 or shRNA–scrambled delivered via TVI at week 8, as indicated. (E) Serum levels of AST and ALT. (F) Representative microphotographs of H&E (upper panel), Oil Red O (middle panel) and Sirius Red staining (lower panel) of liver sections. Lipids in Oil Red O-stained sections and collagen deposition in Sirius Red stained sections (pink area) were quantified using ImageJ. Hepatic triglyceride content was also directly measured. (G) Hepatic protein levels of lipid metabolism markers. (H) Liver proteins levels of PGC1α and SIRT1. (I) Liver protein levels of OXPHOS complex subunits I–V. (J) Complex II activity in liver. (K) Hepatic palmitate oxidation rate (partial and complete oxidation). GAPDH and HPRT were used to normalize protein and mRNA levels, respectively. Dividing lines indicate splicing in the same gel. Data are presented as mean ± SEM; $^{*}p$ <0.05, $^{**}p$ <0.01, $^{***}p$ <0.001, using a Student's *t* test (n = 7–15 per group). ASM, acid soluble metabolites; CDHFD, choline-deficient high-fat diet; OXPHOS, oxidative phosphorylation; sh(RNA), short-hairpin (RNA); TVI, tail vein injection.

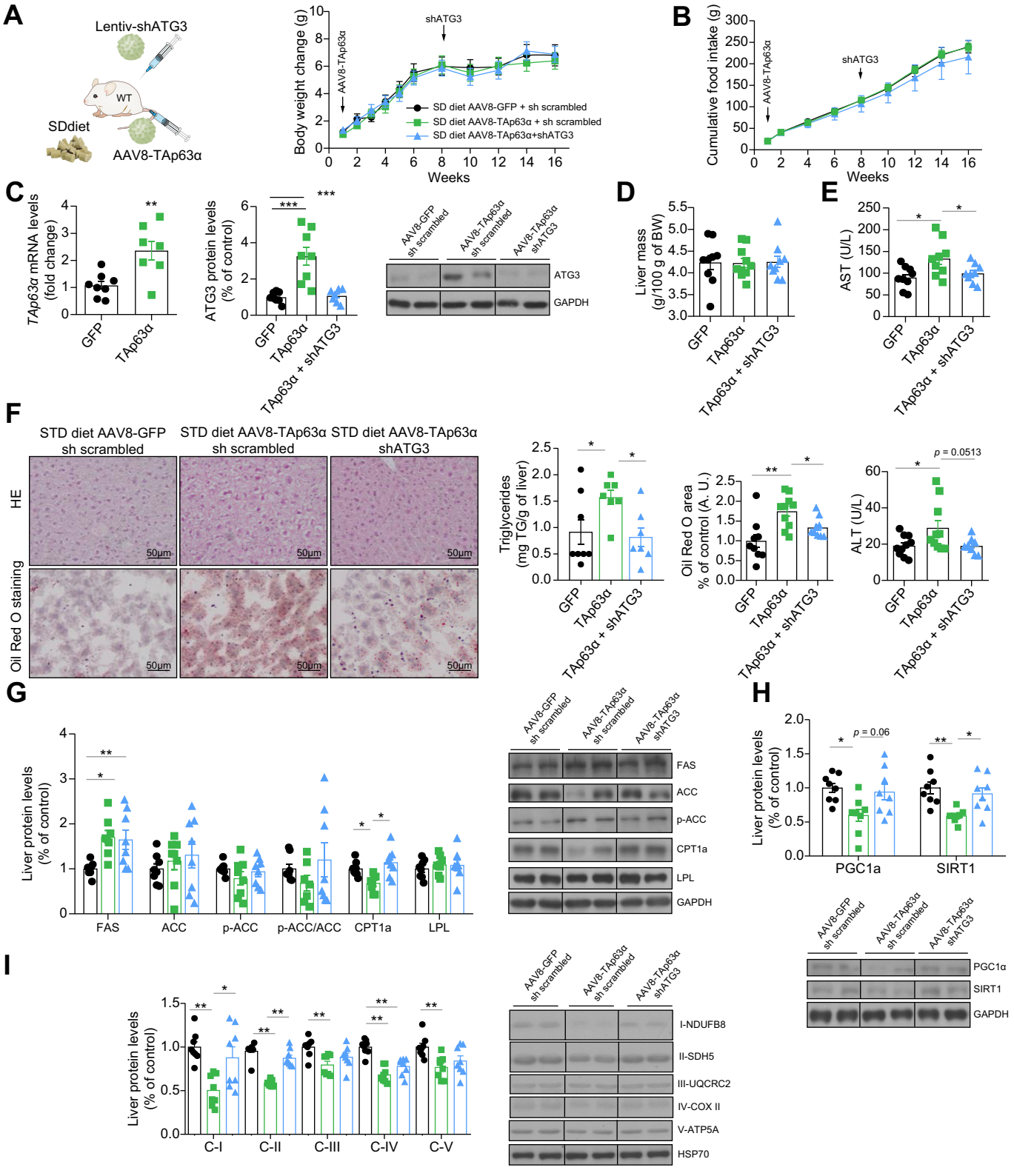

Fig. 6. Liver-specific downregulation of ATG3 ameliorated NAFLD induced by TAp63α. (A) Body weight change, (B) food intake, (C) hepatic levels of TAp63α mRNA and ATG3 protein, and (D) liver mass of mice fed a SD for 16 weeks, with TVI of AAV8–TAp63α or AAV8–GFP at week 1, and a second TVI of lentivirus encoding the shRNA-ATG3 or shRNA-scrambled control at week 8, as indicated. (E) Serum levels of AST and ALT. (F) Representative microphotographs of H&E (upper panel) and Oil Red O staining (lower panel) of liver sections. Oil Red O-stained sections were quantified using ImageJ. Hepatic triglyceride content was also directly measured. (G) Hepatic protein levels of lipid metabolism markers. (H) Liver protein levels of PGC1α and SIRT1. (I) Liver protein levels of OXPHOS complex subunits I–V. Protein levels were normalized to GAPDH and HPS70, and mRNA levels, to HPRT. Dividing lines indicate splicing in the same gel. Data are presented as mean ± SEM; *p <0.05, **p <0.01, using one-way ANOVA followed by a Newman-Keuls Multiple comparison test (n = 7–10 per group). AAV, adeno-associated virus; NAFLD, non-alcoholic fatty liver disease; OXPHOS, oxidative phosphorylation; SD, standard diet; sh(RNA), short-hairpin (RNA); TA, transactivation domain; TVI, tail vein injection.

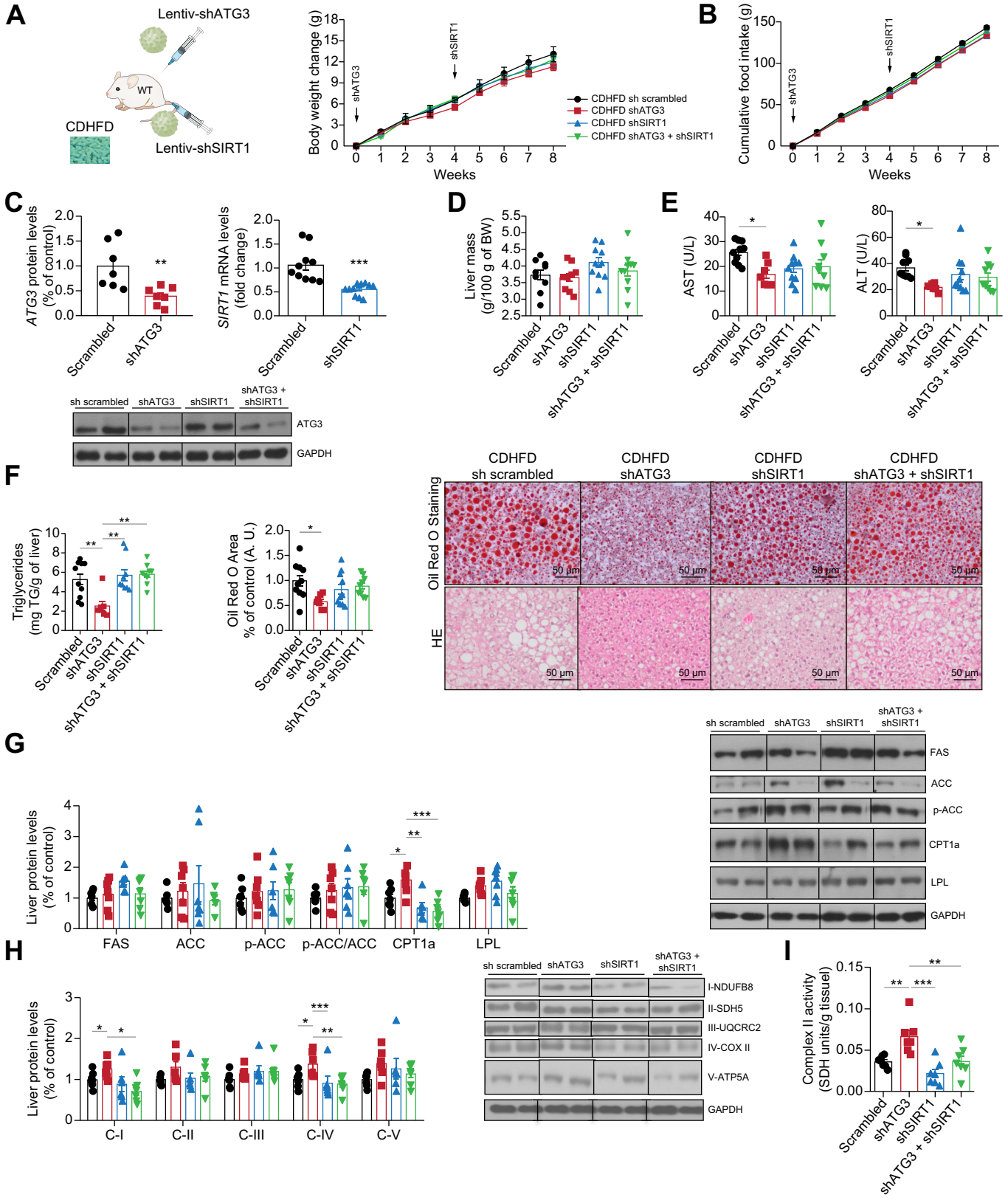

Fig. 7. Inhibition of SIRT1 blunts the effects of liver-specific downregulation of ATG3 in NAFLD. (A) Body weight change, (B) food intake, (C) hepatic levels of ATG3 protein and *SIRT1* mRNA, and (D) liver mass in mice fed CDHFD for 8 weeks, with a lentivirus with shRNA-ATG3 or shRNA-scrambled at week 1, and a second TVI of lentivirus with shRNA-SIRT1 or shRNA-scrambled at week 4, as indicated. (E) Serum levels of AST and ALT. (F) Representative microphotographs of Oil Red O (upper panel) and H&E staining (lower panel) of liver sections. Oil Red O staining was quantified using ImageJ. Hepatic triglyceride content was also directly measured. (G) Hepatic protein levels of lipid metabolism markers. (H) Liver protein levels of OXPHOS complex subunits I–V. (I) Hepatic Complex II activity. Protein levels were normalized with GAPDH, and mRNA levels, with HPRT. Dividing lines indicate splicing in the same gel. *p <0.05, **p <0.01, ***p <0.001, using one-way ANOVA followed by a Newman-Keuls Multiple Comparison Test (n = 9–10 per group). CDHFD, choline-deficient high-fat diet; NAFLD, non-alcoholic fatty liver disease; OXPHOS, oxidative phosphorylation; sh(RNA), short-hairpin (RNA); TVI, tail vein injection.

(Fig. 7D-7E). The reduced lipid content and hepatic triglycerides in mice with ATG3-knockdown was blunted when SIRT1 was subsequently inhibited (Fig. 7F). The knockdown of hepatic ATG3 caused an increase in CPT1a protein levels as well as a higher activity of complex II, but these effects were blocked by co-silencing ATG3 and SIRT1 (Fig. 7G-7I). On the other hand, the expression of fibrotic markers remained unchanged between the groups (Fig. S4C).

ATG3 regulates protein levels of SIRT1 via JNK1

A key factor in regulating SIRT1 protein levels is c-Jun N-terminal kinase 1 (JNK1), whose activation induces SIRT1 protein degradation,[10] while JNK2 induces SIRT1 protein stability.[11] We measured JNK1 and JNK2 in the liver of mice fed a CDHFD where ATG3 was knocked down in the liver and detected reduced levels of JNK1 but not JNK2 (Fig. S10A). Consistent with *in vivo* data, silencing ATG3 in THLE2 cells reduced JNK1 (Fig. S10B), while the induction of ATG3 increased JNK1 (Fig. S10C). Silencing ATG3 in primary hepatocytes decreased JNK1 (Fig. S10D), while its overexpression increased JNK1 (Fig. S10E). Finally, treatment of isolated hepatocytes with the JNK1 inhibitor SP600125 blunted the ATG3-induced actions, including increased lipid content, reduced oxygen consumption rate and SIRT1 activity (Fig. S10F-10H). Although a previous report found that modulation of ATG3 in the adipose tissue activates the Nrf2/Keap1 signaling pathway in the liver,[12] the expression of Nrf2 and Keap1 in the white adipose tissue and liver of mice fed a CDHFD where ATG3 was knocked down remained unaltered (Fig. S11A-11C). Similar results were found in the white adipose tissue of mice where Tap63α was manipulated (Fig. S11D) and in isolated hepatocytes after silencing ATG3 (Fig. S11E).

ATG3 requires CPT1a to modulate lipid metabolism and mitochondrial activity

CPT1a floxed mice fed a CDHFD were injected with AAV8-GFP (control) or AAV8-Cre; at week 4, experimental groups were injected with either scrambled shRNA (control) or shRNA-ATG3, and mice were sacrificed at week 8. Body weight remained unchanged (Fig. S12A). CPT1a and ATG3 levels in livers were reduced after AAV8-Cre or shRNA-ATG3 treatment, respectively (Fig. S12B). Liver mass was not affected, but AST and ALT levels were lower after ATG3-knockdown; these levels returned to baseline when both ATG3 and CPT1a were silenced (Fig. S12C-12D). The reduced lipid and hepatic triglyceride content and increased levels of complex II and IV in mice with ATG3 down-regulation were blunted when CPT1a was also reduced (Fig. S12E-12F). The expression of fibrotic markers was not altered between these groups (Fig. S12G).

ATG3 regulates hepatic lipid content in an autophagy-independent manner

To further explore whether ATG3 exerts its hepatic actions via an autophagy-dependent process, we used both THLE2 and HepG2 hepatocyte cell lines to manipulate ATG3. Upon induction of autophagy, microtubule-associated protein 1 light chain 3 alpha (MAP1LC3A or LC3) is lipidated, and this LC3-phospholipid conjugate (LC3-II) is recruited to autophagosomal membranes and fuses with lysosomes to form autolysosomes, which degrade intra-autophagosomal components and LC3-II.[13,14] As expected, silencing ATG3 in HepG2 cells decreased LC3-II levels (Fig. 8A). We then monitored the autophagic flux by analyzing LC3-II turnover, in the presence or absence of the inhibitor of lysosome-mediated proteolysis, chloroquine (CQ). CQ administration induced the expected LC3-II accumulation (Fig. 8A). Hepatocytes treated with OA and transfected with siATG3 stored fewer lipids, and CQ treatment increased the lipid content (Fig. 8B). Strikingly, however, in cells overexpressing ATG3, inhibition of autophagy by CQ did not affect ATG3-induced lipid droplets in THLE2 or HepG2 cells (Fig. 8C-8D). Thus, these results suggested that the lipid accumulation induced by ATG3 is independent of autophagy. This was confirmed *in vivo*, as ATG3-knockdown in our 2 animal models of steatosis (induced by TAp63α or CDHFD) reduced LC3-II accumulation but did not affect protein and mRNA levels of well-established markers of autophagy such as ATG5, ATG7, and p62 (Fig. 8E-8F). Overall, these data indicate that the effects of ATG3 on lipid content are independent of its autophagic action. This is also supported by the fact that autophagy contributes to the turnover of lipid droplets, and thereby to an increased fatty acid oxidation, a process named lipophagy.[15,16]

Discussion

In this work, we identified for first the time the role of ATG3 on fatty acid metabolism and its implications in the development of NAFLD. ATG3 is elevated in the liver of animal models as well as patients with NAFLD. Moreover, *in vitro* and *in vivo* genetic functional studies indicated that the overexpression of ATG3 favors lipid deposition, while its silencing alleviates steatosis induced by OA, p63, or diet. These novel findings expand our knowledge about the molecular mechanisms involved in liver steatosis.

Autophagy has a well-established role in hepatic lipid metabolism, insulin sensitivity, and cellular injury, suggesting different potential mechanistic roles for autophagy in NAFLD.[17,18] Our initial hypothesis was that ATG3, an enzyme that catalyzes the LC3 lipidation process essential for autophagocytosis,[19] exerts its effects through an autophagic action, as p63 (as well as its family co-members p53 and p73) can induce autophagy.[20,21] Contrary to our expectations, we found that ATG3 modulates lipid metabolism via non-autophagic mechanisms but in a JNK1- and SIRT1-dependent manner. ATG3 increases JNK1 protein levels, which are known to induce SIRT1 protein degradation.[10] The lower protein levels of SIRT1, concomitant to its inhibited activity in human hepatocytes and murine liver reduced fatty acid oxidation and mitochondrial function, leading to a higher lipid load. In agreement with this, the inhibition of ATG3 decreased JNK1 and increased protein levels of SIRT1 and mitochondrial function, ultimately decreasing lipid content. Indeed, many reports have demonstrated a key role of SIRT1 in stimulating mitochondrial function[22] and fatty acid oxidation,[23,24] which contribute to attenuating hepatic steatosis.[25] Our findings show that the protection against steatosis induced by the inhibition of ATG3 was lost when SIRT1 and CPT1a were also suppressed in cells and mice, indicating a functional role for SIRT1 and CPT1a in the anti-steatotic action, which was not associated with changes in autophagic flux. Our results in the liver are opposite to the actions of ATG3 in adipose tissue, where depletion of ATG3 triggered the Nrf2/Keap1 pathway in the liver.[12] However, it is important to note that mice lacking ATG3 in adipose tissue displayed increased adipose tissue inflammation, systemic insulin resistance and accumulation of lipid peroxides, which are known to cause a marked impact on liver metabolism.

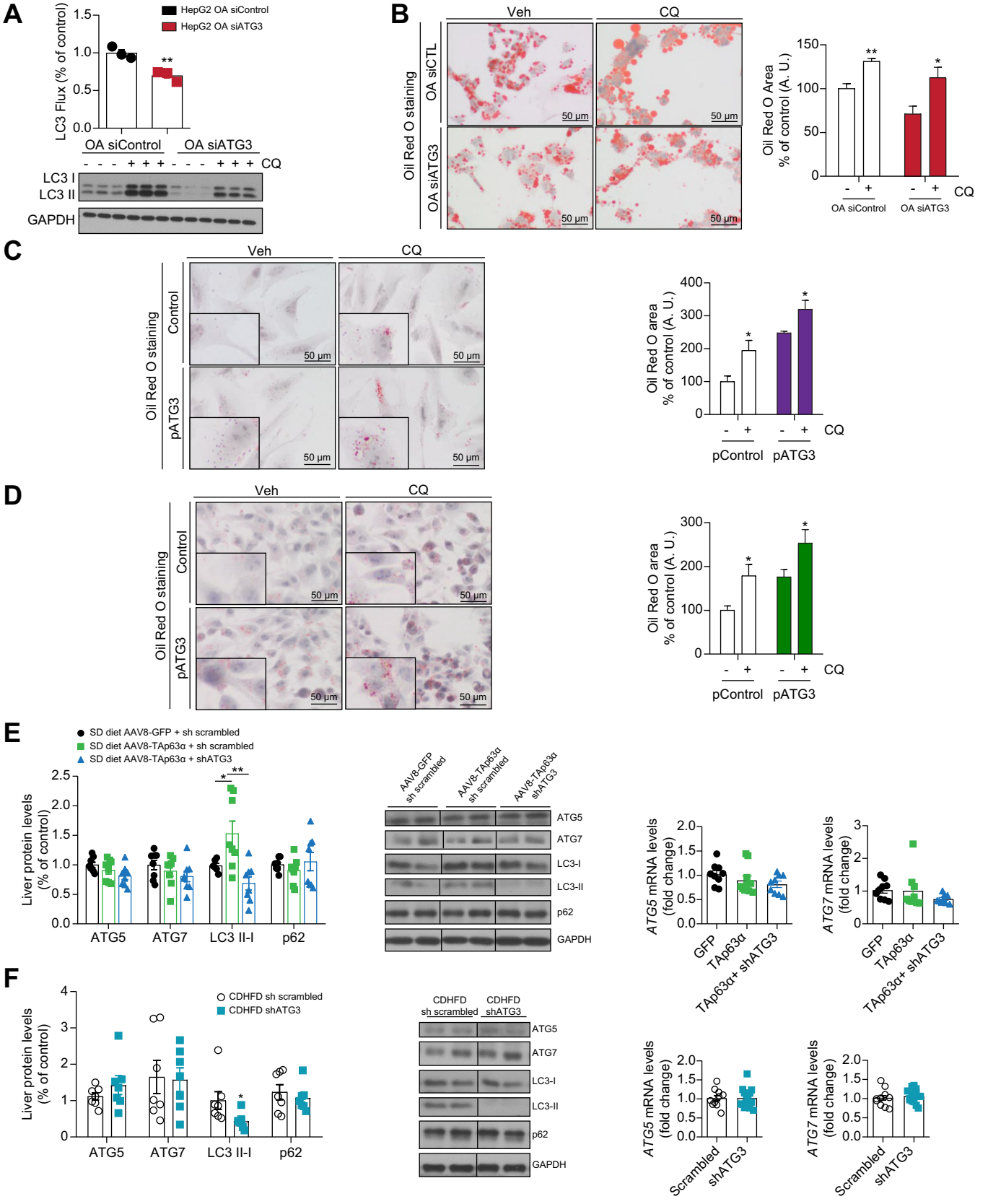

Fig. 8. ATG3 regulates hepatic lipid accumulation in an autophagy-independent manner. HepG2 cells silencing ATG3 were treated for 24 hours with 1 mM OA and 60 μM CQ (added 18 h after OA) (n = 3-4 per group). (A) LC3-I and LC3-II protein levels. (B) Representative microphotographs of Oil Red O staining. Oil Red O staining was quantified using ImageJ and normalized to the total number of nuclei per field. (C) HepG2 cells and (D) THLE2 cells overexpressing ATG3 were

On the other hand, it has also been reported that there is a tissue-specific autophagy response.[26–28]

It is important to highlight that most, if not all, components of the molecular machinery for autophagy mediate effects that do not depend on lysosomal degradation of autophagy substrates.[29,30] Consequently, numerous, distinct non-autophagic biological functions for different ATG proteins have been reported, including cell survival, modulation of cellular transport, secretory processes, signaling, transcriptional/translational responses, and membrane reorganization.[29,30] More specifically, ATG3 has been shown to modulate in an autophagic-independent manner diverse cellular processes such as phagocytosis, secretion and exocytosis and cell proliferation.[30] Our study indicating that the effects of ATG3 are modulated by JNK1, SIRT1 and CPT1a points to another, previously undescribed non-autophagic action. Importantly, our results also propose that different ATGs have opposite actions in the liver, at least in terms of fatty liver disease. While we demonstrated that inhibition of ATG3 ameliorates NAFLD, liver-specific deletion of ATG5, ATG7, or ATG14 exacerbate the susceptibility of mice to develop NAFLD in response to a HFD.[31–34] However, the loss of autophagic factors does not always involve negative actions. For example, mice lacking ATG5 specifically in the liver are protected against acetaminophen-induced liver injury.[35] These paradoxical actions of autophagy might occur after long periods in response to cellular compensatory mechanisms.

The ameliorated steatosis after ATG3-knockdown, and subsequent increased SIRT1 and CPT1a protein levels, was associated with stimulated mitochondrial function. The link between ATG3 and mitochondrial homeostasis has been studied before in the context of cell death, pluripotency acquirement, and maintenance of embryonic stem cells.[36,37] Although those studies suggested that the effects of ATG3 on mitochondria are dependent on autophagy, disruption of ATG3/ATG12 conjugation does not affect starvation-induced autophagy,[37] supporting an autophagic-independent role of ATG3.

In addition to the unexpected mechanism used by ATG3, another important feature is that ATG3 levels are elevated in the livers of different animal models and patients with steatosis and NASH, while its genetic inhibition in mice only alleviated steatosis but did not alter fibrosis. Although ATG3 does not seem to be differentially expressed in the late stages of NAFLD compared to initial phases, it is important to consider that a fraction of people with NAFL will develop NASH or advanced liver fibrosis,[38–40] implying that specific signaling mechanisms are involved in liver disease progression. Considering that ATG3 overexpression is an early dysregulated mechanism and that levels of ATG3 remain high during advanced NASH, it could be of interest for diagnosis and/or as a therapeutic target to prevent the progression of the disease.

In summary, our findings show for the first time that: a) ATG3 expression increased in the liver of mouse models and of patients with NAFLD, who also show a positive correlation between ATG3 with steatosis grade and NAFLD activity score; b) ATG3 overexpression induced lipid load, and its inhibition in the liver ameliorated TAp63α- and diet-induced liver steatosis; c) this anti-steatotic action is mediated by reduction of JNK1 and increased levels of SIRT1, CPT1a, fatty acid oxidation, and mitochondrial function, in an autophagic-independent manner (Fig. S13). Overall, our results point towards ATG3 as a novel molecule implicated in the development of steatosis.

Abbreviations

AAV, adeno-associated virus; ALT, alanine aminotransferase; AST, aspartate aminotransferase; ATG3, autophagy-related gene 3; CDHFD, choline-deficient high-fat diet; CPT1a, carnitine palmitoyltransferase 1a; CQ, chloroquine; DIO, diet-induced obese; FAS, fatty acid synthase; HFD, high-fat diet; JNK1/2, c-Jun N-terminal protein kinase 1/2; LC3 (MAP1LC3A), microtubule-associated protein 1 light chain 3 alpha; LC3-II, LC3-phospholipid conjugate; NAFL, non-alcoholic fatty liver; NAFLD, non-alcoholic fatty liver disease; NASH, non-alcoholic steatohepatitis; OA, oleic acid; PGC1α, proliferator-activated receptor gamma coactivator 1 alpha; SD, standard diet; shRNA, short-hairpin RNA; siRNA, small-interfering RNA; SIRT1, sirtuin 1; TA, transactivation domain.

Financial support

This work has been supported by grants from FEDER/Ministerio de Ciencia, Innovación y Universidades-Agencia Estatal de Investigación (PA: RTI2018-095134-B-100; DS and LH: SAF2017-83813-C3-1-R; MLMC: RTC2019-007125-1; CD: BFU2017-87721; ML: RTI2018–101840-B-I00; GS; PID2019-104399RB-I00; RN: RTI2018-099413-B-I00 and RED2018-102379-T; MLMC: SAF2017-87301-R; TCD: RTI2018-096759-A-100), FEDER/Instituto de Salud Carlos III (AGR: PI19/00123), Xunta de Galicia (ML: 2016-PG068; RN: 2015-CP080 and 2016-PG057), Fundación BBVA (RN, GS and MLM), Proyectos Investigación en Salud (MLMC: DTS20/00138), Sistema Universitario Vasco (PA: IT971-16); Fundación Atresmedia (ML and RN), Fundación La Caixa (M.L., R.N. and M.C.), Gilead Sciences International Research Scholars Program in Liver Disease (MVR), Marató TV3 Foundation (DS: 201627), Government of Catalonia (DS: 2017SGR278) and European Foundation for the Study of Diabetes (RN and GS). This research also received funding from the European Community's H2020 Framework Programme (ERC Synergy Grant-2019-WATCH- 810331, to RN, VP and MS). Centro de Investigación Biomédica en Red (CIBER) de Fisiopatología de la Obesidad y Nutrición (CIBERobn), Centro de Investigación Biomédica en Red (CIBER) de Enfermedades Hepáticas y Digestivas (CIBERehd) and CIBER de Diabetes y Enfermedades Metabólicas Asociadas (CIBERdem). CIBERobn, CIBERehd and CIBERdem are initiatives of the Instituto de Salud Carlos III (ISCIII) of Spain which is supported by FEDER funds. We thank MINECO for the Severo Ochoa Excellence Accreditation to CIC bioGUNE (SEV-2016-0644).

treated for 24 hours with 1 mM OA and 60 μM CQ (added 18 h after OA) (n = 4-7 per group). Representative microphotographs of Oil Red O staining. The n represents the number of independent experiments. (E) Protein levels of autophagy markers and mRNA levels of *ATG5* and *ATG7* in the livers of mice fed a SD with a TVI of AAV8-TAp63α or AAV8-GFP at week 1, and a second TVI of lentivirus with shRNA-ATG3 or shRNA-scrambled at week 8 (n=7-10 per group); and in liver of mice fed a CDHFD with hepatic ATG3 downregulation (n = 7-15 per group) (F). Protein levels were normalized with GAPDH, and mRNA levels, with HPRT. Dividing lines indicate splicing in the same gel. Data are presented as mean ± SEM; *p <0.05, **p <0.01, using a Student's t test (A) (B) (C) (D) (F) or one-way ANOVA followed by a Newman-Keuls Multiple Comparison Test (E). AAV, adeno-associated virus; CDHFD, choline-deficient high-fat diet; CQ, chloroquine; OA, oleic acid; SD, standard diet; sh(RNA), short-hairpin (RNA); TVI, tail vein injection.

Conflict of interest

The authors declare that they have no conflicts of interest related to the study.

Please refer to the accompanying ICMJE disclosure forms for further details.

Authors' contributions

N.D.S.L., M.F.F., E.N., X.B., S.G., M.J.G.-R., U.F., A.L., M.G-V., M.D.P. C-V., S.B.B., P.M., A. E., M.L., D.G., M.F., P.G., M.C., G.S., M. V-R., T.C.D., M.S., R.G.: study conception and design, data acquisition, and data analysis and interpretation; M.L., C.D., L.H., D.S., M.L.M.-C., M.R-G., V.P., C.G-C., A.G-R., P.A., R.N.: manuscript writing and final review.

Data availability statement

The data associated with this paper are available upon request to the corresponding author.

Supplementary data

Supplementary data to this article can be found online at https://doi.org/10.1016/j.jhep.2021.09.008.

References

Author names in bold designate shared co-first authorship

[1] Yang A, Kaghad M, Wang Y, Gillett E, Fleming MD, Dotsch V, et al. p63, a p53 homolog at 3q27-29, encodes multiple products with transactivating, death-inducing, and dominant-negative activities. Mol Cell 1998;2:305–316.

[2] Porteiro B, Fondevila MF, Delgado TC, Iglesias C, Imbernon M, Iruzubieta P, et al. Hepatic p63 regulates steatosis via IKKbeta/ER stress. Nat Commun 2017;8:15111.

[3] Amir M, Czaja MJ. Autophagy in nonalcoholic steatohepatitis. Expert Rev Gastroenterol Hepatol 2011;5:159–166.

[4] **Singh R**, **Kaushik S**, Wang Y, Xiang Y, Novak I, Komatsu M, et al. Autophagy regulates lipid metabolism. Nature 2009;458:1131–1135.

[5] **Yang L**, **Li P**, Fu S, Calay ES, Hotamisligil GS. Defective hepatic autophagy in obesity promotes ER stress and causes insulin resistance. Cell Metab 2010;11:467–478.

[6] Thoen LF, Guimaraes EL, Dolle L, Mannaerts I, Najimi M, Sokal E, et al. A role for autophagy during hepatic stellate cell activation. J Hepatol 2011;55:1353–1360.

[7] Kleiner DE, Brunt EM, Van Natta M, Behling C, Contos MJ, Cummings OW, et al. Design and validation of a histological scoring system for nonalcoholic fatty liver disease. Hepatology 2005;41:1313–1321.

[8] Gerhart-Hines Z, Rodgers JT, Bare O, Lerin C, Kim SH, Mostoslavsky R, et al. Metabolic control of muscle mitochondrial function and fatty acid oxidation through SIRT1/PGC-1alpha. EMBO J 2007;26:1913–1923.

[9] Fondevila MF, Fernandez U, Gonzalez-Rellan MJ, Da Silva Lima N, Buque X, Gonzalez-Rodriguez A, et al. The L-alpha-lysophosphatidylinositol/GPR55 system induces the development of non-alcoholic steatosis and steatohepatitis. Hepatology 2020.

[10] Gao Z, Zhang J, Kheterpal I, Kennedy N, Davis RJ, Ye J. Sirtuin 1 (SIRT1) protein degradation in response to persistent c-Jun N-terminal kinase 1 (JNK1) activation contributes to hepatic steatosis in obesity. J Biol Chem 2011;286:22227–22234.

[11] Ford J, Ahmed S, Allison S, Jiang M, Milner J. JNK2-dependent regulation of SIRT1 protein stability. Cell Cycle 2008;7:3091–3097.

[12] Cai J, Pires KM, Ferhat M, Chaurasia B, Buffolo MA, Smalling R, et al. Autophagy ablation in adipocytes induces insulin resistance and reveals roles for lipid peroxide and Nrf2 signaling in adipose-liver crosstalk. Cell Rep 2018;25:1708–1717 e1705.

[13] Nakatogawa H. Mechanisms governing autophagosome biogenesis. Nat Rev Mol Cell Biol 2020;21:439–458.

[14] **Tsuboyama K**, **Koyama-Honda I**, Sakamaki Y, Koike M, Morishita H, Mizushima N. The ATG conjugation systems are important for degradation of the inner autophagosomal membrane. Science 2016;354:1036–1041.

[15] Mizushima N, Levine B, Cuervo AM, Klionsky DJ. Autophagy fights disease through cellular self-digestion. Nature 2008;451:1069–1075.

[16] Martinez-Lopez N, Singh R. Autophagy and lipid droplets in the liver. Annu Rev Nutr 2015;35:215–237.

[17] Hazari Y, Bravo-San Pedro JM, Hetz C, Galluzzi L, Kroemer G. Autophagy in hepatic adaptation to stress. J Hepatol 2020;72:183–196.

[18] Ueno T, Komatsu M. Autophagy in the liver: functions in health and disease. Nat Rev Gastroenterol Hepatol 2017;14:170–184.

[19] Fujita N, Itoh T, Omori H, Fukuda M, Noda T, Yoshimori T. The Atg16L complex specifies the site of LC3 lipidation for membrane biogenesis in autophagy. Mol Biol Cell 2008;19:2092–2100.

[20] Napoli M, Flores ER. The family that eats together stays together: new p53 family transcriptional targets in autophagy. Genes Dev 2013;27:971–974.

[21] Kenzelmann Broz D, Spano Mello S, Bieging KT, Jiang D, Dusek RL, Brady CA, et al. Global genomic profiling reveals an extensive p53-regulated autophagy program contributing to key p53 responses. Genes Dev 2013;27:1016–1031.

[22] Tang BL. Sirt1 and the mitochondria. Mol Cells 2016;39:87–95.

[23] Gillum MP, Erion DM, Shulman GI. Sirtuin-1 regulation of mammalian metabolism. Trends Mol Med 2011;17:8–13.

[24] Nogueiras R, Habegger KM, Chaudhary N, Finan B, Banks AS, Dietrich MO, et al. Sirtuin 1 and sirtuin 3: physiological modulators of metabolism. Physiol Rev 2012;92:1479–1514.

[25] Li Y, Wong K, Giles A, Jiang J, Lee JW, Adams AC, et al. Hepatic SIRT1 attenuates hepatic steatosis and controls energy balance in mice by inducing fibroblast growth factor 21. Gastroenterology 2014;146:539–549 e537.

[26] Chapin HC, Okada M, Merz AJ, Miller DL. Tissue-specific autophagy responses to aging and stress in C. elegans. Aging (Albany NY) 2015;7:419–434.

[27] Marino G, Salvador-Montoliu N, Fueyo A, Knecht E, Mizushima N, Lopez-Otin C. Tissue-specific autophagy alterations and increased tumorigenesis in mice deficient in Atg4C/autophagin-3. J Biol Chem 2007;282:18573–18583.

[28] Singh R. Autophagy and regulation of lipid metabolism. Results Probl Cell Differ 2010;52:35–46.

[29] Subramani S, Malhotra V. Non-autophagic roles of autophagy-related proteins. EMBO Rep 2013;14:143–151.

[30] Galluzzi L, Green DR. Autophagy-independent functions of the autophagy machinery. Cell 2019;177:1682–1699.

[31] Hammoutene A, Biquard L, Lasselin J, Kheloufi M, Tanguy M, Vion AC, et al. A defect in endothelial autophagy occurs in patients with non-alcoholic steatohepatitis and promotes inflammation and fibrosis. J Hepatol 2020;72:528–538.

[32] Xiong X, Tao R, DePinho RA, Dong XC. The autophagy-related gene 14 (Atg14) is regulated by forkhead box O transcription factors and circadian rhythms and plays a critical role in hepatic autophagy and lipid metabolism. J Biol Chem 2012;287:39107–39114.

[33] Liu K, Zhao E, Ilyas G, Lalazar G, Lin Y, Haseeb M, et al. Impaired macrophage autophagy increases the immune response in obese mice by promoting proinflammatory macrophage polarization. Autophagy 2015;11:271–284.

[34] Ni HM, Woolbright BL, Williams J, Copple B, Cui W, Luyendyk JP, et al. Nrf2 promotes the development of fibrosis and tumorigenesis in mice with defective hepatic autophagy. J Hepatol 2014;61:617–625.

[35] Ni HM, Boggess N, McGill MR, Lebofsky M, Borude P, Apte U, et al. Liver-specific loss of Atg5 causes persistent activation of Nrf2 and protects against acetaminophen-induced liver injury. Toxicol Sci 2012;127:438–450.

[36] Liu K, Zhao Q, Liu P, Cao J, Gong J, Wang C, et al. ATG3-dependent autophagy mediates mitochondrial homeostasis in pluripotency acquirement and maintenance. Autophagy 2016;12:2000–2008.

[37] Radoshevich L, Murrow L, Chen N, Fernandez E, Roy S, Fung C, et al. ATG12 conjugation to ATG3 regulates mitochondrial homeostasis and cell death. Cell 2010;142:590–600.

[38] McPherson S, Hardy T, Henderson E, Burt AD, Day CP, Anstee QM. Evidence of NAFLD progression from steatosis to fibrosing-steatohepatitis using paired biopsies: implications for prognosis and clinical management. J Hepatol 2015;62:1148–1155.

[39] Adams LA, Ratziu V. Non-alcoholic fatty liver - perhaps not so benign. J Hepatol 2015;62:1002–1004.

[40] Pais R, Charlotte F, Fedchuk L, Bedossa P, Lebray P, Poynard T, et al. A systematic review of follow-up biopsies reveals disease progression in patients with non-alcoholic fatty liver. J Hepatol 2013;59:550–556.